PHILOSOPHICAL TRANSACTIONS OF THE ROYAL SOCIETY A

Phil. Trans. R. Soc. A (2010) **368**, 2395–2415
doi:10.1098/rsta.2010.0053

Review

A Palaeogene perspective on climate sensitivity and methane hydrate instability

By T. Dunkley Jones[1,4,*], A. Ridgwell[2], D. J. Lunt[2], M. A. Maslin[1], D. N. Schmidt[3] and P. J. Valdes[2]

[1]*Department of Geography, University College London, London, UK*
[2]*School of Geographical Sciences, and* [3]*Department of Earth Sciences, University of Bristol, Bristol, UK*
[4]*Department of Earth Science and Engineering, Imperial College London, London SW7 2AZ, UK*

The Palaeocene–Eocene thermal maximum (PETM), a rapid global warming event and carbon-cycle perturbation of the early Palaeogene, provides a unique test of climate and carbon-cycle models as well as our understanding of sedimentary methane hydrate stability, albeit under conditions very different from the modern. The principal expression of the PETM in the geological record is a large and rapid negative excursion in the carbon isotopic composition of carbonates and organic matter from both marine and terrestrial environments. Palaeotemperature proxy data from across the PETM indicate a coincident increase in global surface temperatures of approximately 5–6°C. Reliable estimates of atmospheric CO_2 changes and global warming through past transient climate events can provide an important test of the climate sensitivities reproduced by state-of-the-art atmosphere–ocean general circulation models. Here, we synthesize the available carbon-cycle model estimates of the magnitude of the carbon input to the ocean–atmosphere–biosphere system, and the consequent atmospheric pCO_2 perturbation, through the PETM. We also review the theoretical mass balance arguments and available sedimentary evidence for the role of massive methane hydrate dissociation in this event. The plausible range of carbon mass input, approximately 4000–7000 PgC, strongly suggests a major alternative source of carbon in addition to any contribution from methane hydrates. We find that the potential range of PETM atmospheric pCO_2 increase, combined with proxy estimates of the PETM temperature anomaly, does not necessarily imply climate sensitivities beyond the range of state-of-the-art climate models.

Keywords: PETM; climate sensitivity; methane hydrate

*Author for correspondence (t.dunkley-jones@imperial.ac.uk).

One contribution of 15 to a Theme Issue ‘Climate forcing of geological and geomorphological hazards’.

1. Introduction

The Palaeocene/Eocene thermal maximum ('PETM'; approx. 55.5 Ma) is the most prominent transient global warming event recorded in the Cenozoic geological record. PETM palaeotemperature proxy data from some localities indicate a rapid surface ocean warming of approximately 5–9°C within 1–10 kyr (Thomas *et al.* 2002; Sluijs *et al.* 2007). Near synchronous with this warming are prominent negative carbon isotopic excursions (CIEs) recorded in both marine carbonates (−3.5 to −4‰; Zachos *et al.* 2007) and terrestrial carbon (−5 to −6‰; Bowen *et al.* 2004), indicative of a massive release of isotopically light carbon to the ocean–atmosphere system (Dickens *et al.* 1995). The PETM offers a unique opportunity to investigate the effects of an anthropogenic-scale (thousands of gigatons) release of greenhouse gases on the Earth's climate, ocean–atmosphere chemistry and biota, although with a release rate at least an order of magnitude slower than that achieved by the modern combustion of fossil fuels and deforestation (Zeebe *et al.* 2009). There were also major differences in the background climate state of the early Palaeogene that preclude a direct comparison with the modern system. These include significantly higher surface- and deep-ocean temperatures, the absence of polar ice sheets (Zachos *et al.* 2008), as well as a distinct palaeogeography, ocean chemistry and biosphere (see Kump *et al.* (2009) for a review).

Despite these caveats, the PETM is a pertinent geological analogue for future global change and can be used to test the behaviour of climate models—such as their simulation of global climate sensitivity—under conditions of extreme warming (Zeebe *et al.* 2009). To assess (past) climate sensitivity—which is generally defined as the equilibrium surface warming in response to a doubling of CO_2 (and/or the equivalent radiative increase from a different greenhouse gas)—both atmospheric CO_2 and the corresponding warming response must be known. In the case of the PETM, there remains considerable uncertainty over (i) the source and magnitude of carbon release, (ii) the size of the PETM atmospheric CO_2 perturbation, and (iii) the magnitude and spatial pattern of the associated climate response. The potential involvement of a massive destablization of methane gas hydrates, driven by a progressive warming of oceanic intermediate waters (Dickens *et al.* 1995), also has a particular relevance within a discussion of the climatic forcing of major geohazards and is a further point of considerable current uncertainty regarding our understanding of the PETM. This paper thus critically reviews two aspects of PETM research that have a particular relevance to modern climate change and the associated climate-forced geohazards: first, the evidence for a global-scale release of methane hydrate at the PETM and, second, the magnitude of global climate sensitivity that can be inferred from the PETM climate–carbon-cycle perturbation.

The involvement of methane hydrates within the PETM climate–carbon-cycle perturbation was first proposed—based on mass-balance arguments—to explain the magnitude of the observed PETM CIE (Dickens *et al.* 1995). Subsequently, some seismic and sedimentological evidence has been published indicating large-scale slope failure along the western margin of the Atlantic basin close to the Palaeocene–Eocene boundary, which may have been associated with the catastrophic dissociation of methane hydrate (Katz *et al.* 1999, 2001). We review these arguments in the light of more recent estimates of the PETM CIE and

the size of the PETM carbon input. The second part of this paper, concerning the quantification of PETM climate sensitivity, reviews the available estimates of both the atmospheric CO_2 concentration (partial pressure) (pCO_2) perturbation and global average surface warming across the event. At present, there is no reliable proxy estimate of pCO_2 change across the PETM. Instead, quantification of the pCO_2 increase (ΔpCO_2) depends on carbon-cycle model estimates of the size of the PETM carbon pulse and the time-dependent partitioning of CO_2 between the atmosphere, ocean and, eventually, carbonate sediments. These model estimates, in turn, rely upon observations from the geological record of the intensity and extent of carbonate dissolution across the PETM as well as the magnitude of the CIE. There are multiple assumptions made throughout this process, as well as inherent variation in the response of different carbon-cycle models. In addition, although direct proxy data are available for the extent of PETM surface warming at multiple locations, the use of these data as an estimate of global surface warming requires care (Dunkley Jones *et al.* in preparation). All of these uncertainties need to be kept in mind when any estimate of PETM climate sensitivity is proposed. This paper draws on an ongoing integrated climate and Earth-system modelling project—the 'Dynamics of the Palaeocene Eocene Thermal Maximum', part of the Natural Environmental Research Council's (NERC) Quantifiying and Understanding Earth Systems through Modelling (QUEST) research programme—that uses a multi-model approach to quantify and reduce the existing uncertainties in the PETM climate and carbon-cycle perturbation.

2. The PETM and methane hydrates

The magnitude and rapidity of the PETM CIE is a critical constraint on the mass and source of carbon injected into the exogenic carbon reservoir during the PETM. With reliable estimates of the mean size of the PETM CIE in the exogenic carbon reservoir, the total mass of this reservoir and an independent estimate of the mass of carbon input, it would be possible to determine the carbon isotopic composition, and hence nature, of the injected carbon using a relatively simple mass balance. Unfortunately, there remains some uncertainty in the magnitude of the PETM CIE, with significant variations in the size of $\delta^{13}C$ excursions recorded in different substrates and across marine/terrestrial environments, and as yet no consistent estimate of the mass of carbon input. To the first order, there appear to be three distinct and generally consistent sets of CIE records: (i) those from deep-sea benthic foraminifera, which should record the $\delta^{13}C$ evolution of deep-ocean dissolved inorganic carbon (DIC), (ii) those from well-preserved planktonic foraminifera, recording the $\delta^{13}C$ of surface ocean DIC, and (iii) terrestrial records, largely controlled by the $\delta^{13}C$ of terrestrial vegetation and hence recording the $\delta^{13}C$ evolution of atmospheric CO_2. The critical question is which of these records most accurately records the pattern and magnitude of the global CIE.

Benthic foraminiferal $\delta^{13}C$ records from deep-ocean cores typically indicate a CIE of the order of -2 to $-3‰$ (Nunes & Norris 2006). The magnitude of the CIE in these pelagic successions is, however, clearly influenced by the extent of carbonate dissolution and the ecological exclusion (through extinction) of calcareous benthic foraminifera across the onset to peak-PETM (Thomas 2007;

McCarren *et al.* 2008). These two effects will both tend to cause the loss of peak negative δ^{13}C values to an extent that is difficult to assess at any single location. Across the Walvis Ridge depth transect, however, there is a clear relation between palaeodepth, and hence dissolution intensity, and CIE magnitude: the CIE recorded in benthic foraminifera declines from −3.5 to −1.5‰ between sites with palaeodepths of approximately 1500 and 3600 m (McCarren *et al.* 2008). This effect partly accounts for the discrepancy between early estimates of the CIE of the order of −2 to −3‰ (Dickens *et al.* 1995) and more recent estimates of −4 to −6‰ (Pagani *et al.* 2006; Zachos *et al.* 2007). To overcome the problem of deep-ocean carbonate dissolution, attention has recently turned to the PETM records from shelf environments. The high sedimentation rates and shallow water depths at these locations combine to provide higher resolution records, particularly of the onset of the PETM, which are less impacted by carbonate dissolution. The planktonic foraminiferal (i.e. surface ocean DIC) δ^{13}C records of the PETM in these locations indicate a CIE of approximately −4‰ (Zachos *et al.* 2006; Handley *et al.* 2008; John *et al.* 2008), a magnitude that is consistent with the largest excursion values recorded in planktonic foraminifera from pelagic sections, such as ODP Site 690, with minimal dissolution (Thomas *et al.* 2002; Zachos *et al.* 2007).

Although the magnitude of the CIE recorded in carbonates from the most complete and well-preserved marine sections appears to be converging on approximately −4‰, there remains a persistent discrepancy between this value and the CIE magnitude of approximately −6‰ recorded across both organic and inorganic carbon phases from the terrestrial biosphere (Bowen *et al.* 2004; Pagani *et al.* 2006; Handley *et al.* 2008). A range of perturbations in the terrestrial environment have been proposed as mechanisms for CIE amplification on land, including changes in soil cycling rates, relative humidity and vegetation (Bowen *et al.* 2004). None of these has yet provided a satisfactory solution to the marine–terrestrial CIE discrepancy. It should be noted that invoking large (approx. 20%) increases in relative humidity as a comprehensive (i.e. global) explanation of the terrestrial CIE amplification (Bowen *et al.* 2004) is inconsistent with both the hydrological response of global climate models (Pagani *et al.* 2006) and much palaeohydrological proxy data (Wing *et al.* 2005; Kraus & Riggins 2007). Given the continuing uncertainty surrounding the controls on the terrestrial CIE, the emerging consensus on the size of the CIE in surface ocean DIC and the dominance of the oceanic carbon pool relative to the terrestrial biosphere and atmospheric carbon (figure 1), we make the conservative assumption that the global exogenic carbon reservoir CIE is of the order of −4‰.

Carbon exchanges rapidly between the Earth's ocean, atmosphere and biomass reservoirs, which on 10^4 year time scales can be considered as a single reservoir with a mean carbon isotopic composition driven by the rate of external inputs or removal of carbon (Dickens 2003). Some deep-ocean records suggest a stratigraphic lag between the onset of the CIE recorded in mixed layer dwelling foraminifera and the onset in deeper dwelling thermocline species (Thomas *et al.* 2002; Zachos *et al.* 2007). The approximately 5 kyr duration of this inferred top–down propagation of the δ^{13}C signal from the surface ocean to the thermocline is, however, contrary to current understanding of ocean physics and circulation, even allowing for enhanced warming-induced stratification. In particular, the recorded δ^{13}C transition at both surface and thermocline depths is abrupt

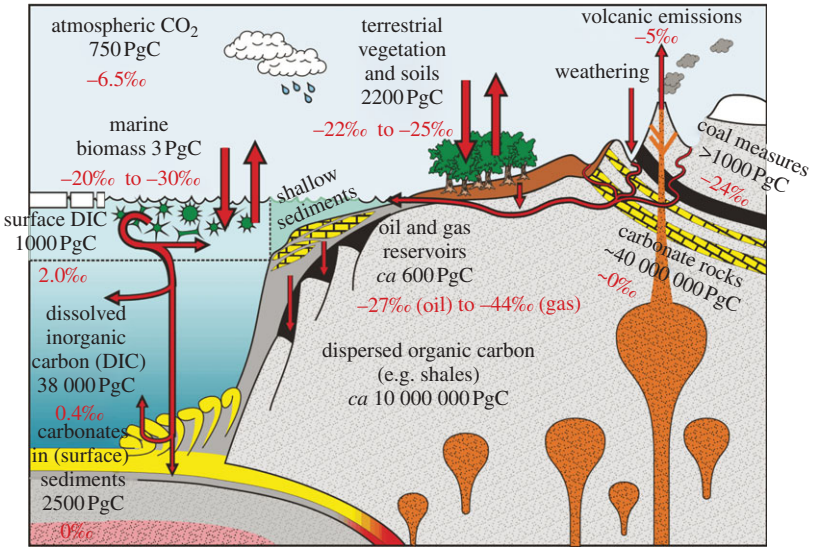

Figure 1. Schematic model of the major exogenic carbon reservoirs within the modern Earth system (after Ridgwell & Edwards 2007).

with no evidence of intermediate values (Thomas *et al.* 2002), whereas the signal expected from a protracted propagation of the CIE anomaly by micro-scale mixing and diffusion should be significantly 'smeared'. Thus, the existence of a secondary species and/or habitat-specific control on the recorded $\delta^{13}C$ patterns seems a more probable explanation, although one which is yet to be understood. Notwithstanding that possibility, there is widespread evidence that the light carbon released at the onset of the PETM was relatively rapidly cycled throughout the whole ocean–atmosphere–biosphere system, with dramatic falls in carbon isotope values recorded across terrestrial, surface-ocean and deep-marine environments within approximately 10 kyr (Bowen *et al.* 2004; Nunes & Norris 2006; Zachos *et al.* 2007).

The size of the PETM CIE thus provides a critical constraint on the source of carbon entering the exogenic reservoir (Dickens *et al.* 1995). Any given $\delta^{13}C$ excursion in the total exogenic carbon reservoir can be simply related to the quantity of mass input and $\delta^{13}C$ signature of the external carbon source,

$$(M_T + M_R)(\delta^{13}C_{T'}) \approx (M_R)(\delta^{13}C_R) + (M_T)(\delta^{13}C_T), \tag{2.1}$$

where M_T and M_R are the masses of carbon in the exogenic reservoir prior to input and the mass of the carbon input; and $\delta^{13}C_R$, $\delta^{13}C_T$, $\delta^{13}C_{T'}$ are the carbon isotopic compositions of the carbon input and the exogenic carbon reservoir before and after mass input. Taking into account the large mass of the total exogenic carbon reservoir, to produce a −4.0‰ PETM $\delta^{13}C$ excursion within approximately 10 kyr, the fluxes from any of the conventional long-term (background) carbon sources, such as volcanic activity, weathering or riverine input, would have to increase at a rate that is geologically unfeasible; for example, a 100-fold increase in the rate of volcanic out-gassing (Dickens *et al.* 1995).

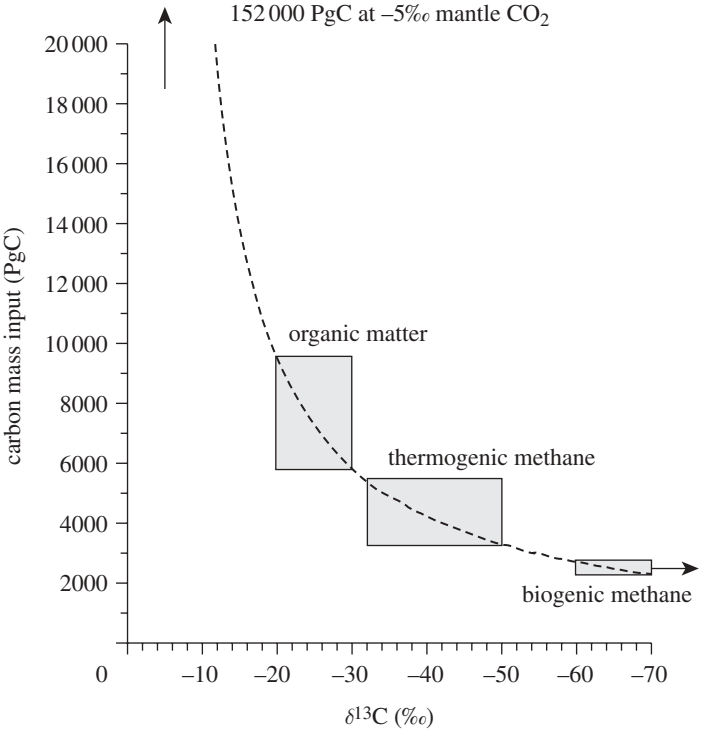

Figure 2. The carbon mass input required to produce a −4‰ CIE within an exogenic carbon reservoir of 38 000 PgC, with carbon sources of varying isotopic composition. Assumes that the mean isotopic composition of the ocean and atmosphere prior to carbon input is 0‰; estimated isotopic values of major sources based upon Maslin & Thomas (2003).

Today, by the burning of fossil fuels and deforestation (Prentice *et al.* 2001), and during the glacial–interglacial cycles of the late Neogene (Kohfeld & Ridgwell 2009), carbon isotopic changes in the atmosphere and ocean are driven primarily through the release of isotopically depleted CO_2 from organic matter, with $\delta^{13}C$ signatures of approximately −26‰ for biospheric carbon (Prentice *et al.* 2001) and approximately −28‰ for fossil fuels (Andres *et al.* 1993). The total mass of carbon necessary to produce the PETM CIE from such a source is, however, problematic. Using estimates from the modern system to produce a −2‰ to −3‰ excursion in the ocean–atmosphere carbon reservoir would require the loss of between 75 and 90 per cent of the total organic carbon reservoir (Dickens *et al.* 1995). To obtain a −4‰ magnitude of excursion requires approximately 8000 PgC for a −22‰ to −24‰ source (figure 2)—a greater loss of organic carbon than exists in the modern carbon cycle. Proposals for the PETM carbon release involving organic matter—the desiccation of shallow epicontinental basins (Higgins & Schrag 2006) and the global-scale combustion of terrestrial peat and coal (Kurtz *et al.* 2003)—hence invoke a larger reservoir prior to the PETM than exists today. Other potential sources exist for carbon of this approximate isotopic composition, such as that released from the impact of a carbon-rich meteorite (Kent *et al.* 2003) and, more plausibly, as thermogenic methane released during volcanic activity in the North Atlantic (Svensen *et al.* 2004).

The difficulties faced in reconciling the isotopic composition of either a volcanic (approx. −5‰) or organic matter (approx. −22‰ to −24‰) carbon source with the magnitude of the PETM CIE imply a significant additional contribution from an extremely ^{13}C-depleted carbon reservoir. In addition, this reservoir has to be outside of the exchangeable ocean–atmosphere–terrestrial carbon cycle and yet be released into the ocean–atmosphere system on time scales of 1–10 kyr. The leading contender for this source of light carbon remains sediment-hosted methane gas hydrates (Dickens *et al.* 1995). In the modern system, methane hydrates are stable under relatively high-pressure/low-temperature conditions and are found within sedimentary prisms along many continental margins, typically associated with both free and dissolved methane gas trapped beneath the hydrate layer (Kvenvolden 1993). The methane present in these deposits, sourced from either the microbial fermentation of organic matter or thermal cracking, typically has a δ^{13}C signature of the order of −60‰ (Kvenvolden 1993). The pressure–temperature–salinity defined region within a sediment column in which gas hydrates are theoretically stable is termed the gas hydrate stability zone (GHSZ), while the actual occupancy of the GHSZ by methane hydrates is determined by the supply of methane, itself dependent on organic carbon burial rates and local redox and fluid flow conditions (see also the review of methane gas hydrates in Maslin *et al.* (2010)). Owing to significantly warmer oceanic intermediate and bottom-water temperatures in the Palaeocene, it is estimated that the upper limit of the Palaeocene GHSZ was located in considerably deeper waters (approx. 900 m) than modern systems (approx. 250–500 m) (Dickens 2003). Despite this, a major decrease in pressure, or more probably an increase in temperature at subthermocline to intermediate water depths, and its propagation down through the sediment geotherm, could have triggered the dissociation of significant portions of a Palaeocene gas hydrate reservoir. In the initial presentation of this hypothesis, Dickens *et al.* (1995) calculated that a 4°C warming on background latest Palaeocene bottom-water temperatures of 11°C would have depressed the top of the GHSZ from approximately 900 m to 1400 m water depth with an associated dissociation of 1000–2000 Pg of methane carbon.

Although the transfer pathways for dissociated methane gas from the GHSZ into the exchangeable carbon reservoir are still poorly understood, the two most likely routes are via diffusion into the water column or ebullition into the atmosphere during sediment failure (Kvenvolden 1993; Paull *et al.* 2003). Once released, this methane would have been rapidly oxidized (<10 years) to carbon dioxide in the oceans (Valentine *et al.* 2001) and atmosphere (Ehhalt *et al.* 2001), which in turn would be relatively rapidly exchanged between the surface and deep ocean, the atmosphere and terrestrial biomass. The dissociation of substantial volumes of gas-hydrate-hosted methane over approximately 10^4 years would have both increased the total mass of the exchangeable carbon reservoir and produced the observed decrease in its mean isotopic composition (Dickens *et al.* 1995).

A critical part of a warming-driven methane hydrate dissociation hypothesis is that intermediate water warming, as the trigger for hydrate destabilization, should lead the observed CIE. There is now some evidence for a precursor warming, at least in surface waters, immediately prior to the onset of the CIE observed in high-resolution continental shelf records of the North Atlantic (Sluijs *et al.* 2007). This finding needs to be substantiated by additional records,

particularly from intermediate water depths. One plausible scenario is that this initial warming is itself a response to rapid emissions of CO_2 from the latest Palaeocene explosive volcanism in either the North Atlantic (Storey *et al.* 2007) or Caribbean (Bralower *et al.* 1997). Recent climate modelling studies, configured to PETM-like boundary conditions, have also shown a strong, nonlinear warming response of Atlantic intermediate waters to such a CO_2 forcing (Lunt *et al.* submitted), providing an amplification of warming in a hydrate-critical region. The presence of major submarine mass movement deposits, of Palaeocene–Eocene boundary age, in the North Atlantic (Katz *et al.* 1999, 2001) adds to the suspicion that massive methane release along Atlantic continental margins could have played a significant role in the PETM event.

3. Magnitude of PETM carbon release

Obtaining a reliable estimate of the total mass input of carbon into the exogenic carbon cycle is critical to understanding the size and rate of carbon fluxes between reservoirs, the magnitude of the perturbation in atmospheric CO_2 and the response of the climate system through the PETM. There are two key constraints on the mass of carbon input at the PETM: the size of the PETM CIE and the degree of sedimentary carbonate dissolution in the deep oceans owing to CO_2-driven carbonate undersaturation. Some theoretical limits on the specific contribution of methane gas hydrates to the PETM event may also be achieved by the predictive modelling of the latest Palaeocene GHSZ and its occupancy by methane hydrates. The massive release of carbon into the ocean/atmosphere system over approximately 10^4 years, the majority being absorbed by the ocean, would have caused significant reductions in both the pH and carbonate ion concentration of the deep ocean (Broecker *et al.* 1971, 1993). This in turn would have increased the dissolution of biogenic carbonates (primarily calcareous nannofossil liths and foraminiferal tests) in the surface sediments of the deep ocean,

$$CO_2 + H_2O + CaCO_3 = 2HCO_3^- + Ca^{2+}.$$

One observable consequence of this is a marked shoaling of both the lysocline and carbonate compensation depth (CCD) across the global oceans (Ridgwell & Zeebe 2005; Kump *et al.* 2009). The magnitude of this dissolution event observed in the geological record is fundamentally controlled by the mass and the rate of carbon input to the ocean–atmosphere system and, within the constraints imposed by the size of the PETM CIE, can be used to estimate the magnitude of the carbon input. In reality, the extent of carbonate dissolution at any given location is also locally regulated by primary carbonate production rates, local deep-water chemistry and the rate of mixing/bioturbation at the sediment surface, which all confound a simple solution to this problem (Ridgwell 2007). The reservoir of carbonate in deep-sea sediments available for reaction is also finite (Archer *et al.* 1997) and the relationship between $CaCO_3$ reacted (chemically eroded) and CO_2 release becomes increasingly nonlinear at CO_2 releases greater than 4000 PgC (Goodwin & Ridgwell in press), requiring global carbon-cycle models to interpret observations.

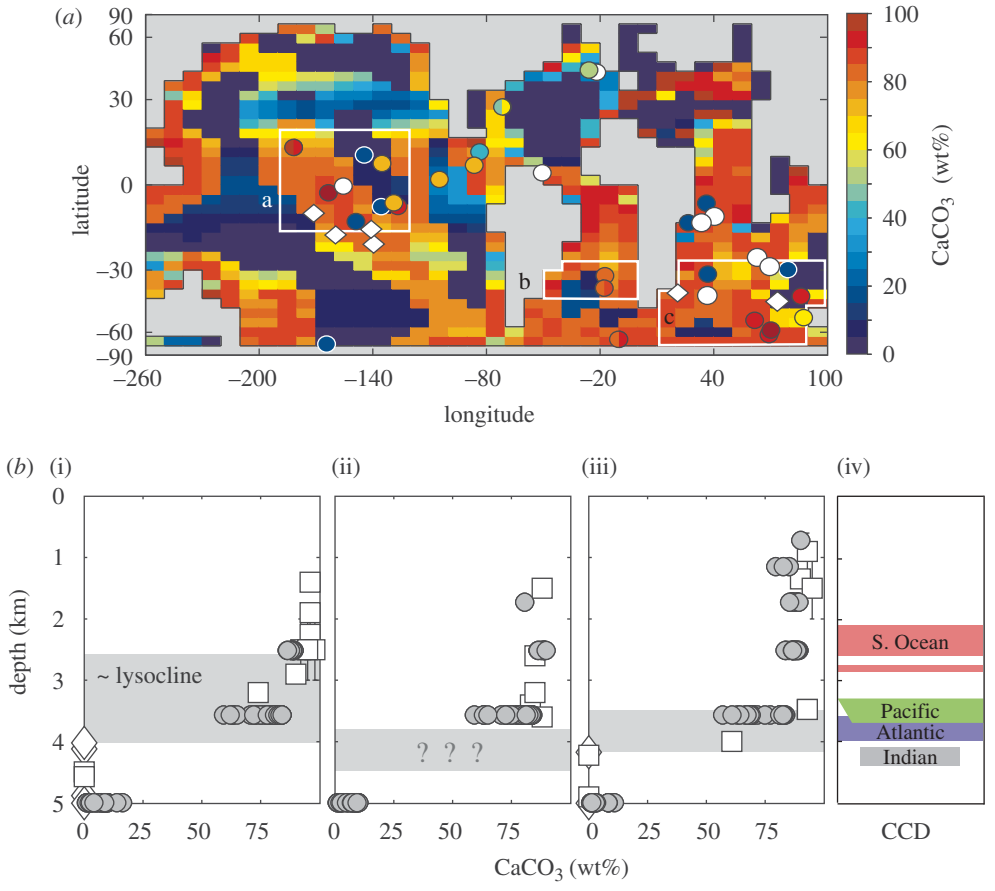

Figure 3. (*a*) Pre-PETM model CaCO3 wt% of Panchuk *et al.* (2008) plotted in map view and versus (*b*) depth, both with observations superimposed. Carbonate variation with depth (below) is plotted for the data-rich regions delineated in (*a*) by white boxes: a, central equatorial Pacific Ocean; b, Walvis Ridge; c, Southern Indian Ocean. (*a*) Yellow filled circle, observed $CaCO_3$ wt%; unfilled circle, $CaCO_3$ present but unknown wt%; unfilled diamond, hiatus. (*b*) (i) Pacific Ocean. (ii) Walvis Ridge. (iii) Indian Ocean. (iv) The pre-PETM CCD reconstructions of Zeebe *et al.* (2009). Grey filled circle, model; unfilled square, data; unfilled diamond, hiatus.

To date, there have been three key studies which aim to quantify the magnitude of the PETM carbon pulse using the extent of deep-ocean carbonate dissolution. The first of these is based on detailed weight percent carbonate and $\delta^{13}C$ analyses of deep-ocean sediment cores from five locations along an approximately 2 km depth transect on Walvis Ridge in the South Atlantic (Zachos *et al.* 2005). These sites effectively provide a vertical profile of carbonate ion concentrations and PETM CCD shoaling through the deep ocean. In addition, the close proximity of all five sites greatly reduces potential biases between these records owing to variations in carbonate export productivity and terrigenous particle flux (Zachos *et al.* 2005). Based on correlations between these sites and the orbital age model at ODP Site 690, the CCD at Walvis Ridge shoaled by more than 2 km in a few thousand years (Zachos *et al.* 2005). By a comparison with numerical models of

anthropogenic-forced ocean acidification and CCD shoaling (Archer *et al.* 1997), Zachos *et al.* (2005) suggest that the PETM carbon pulse required to produce such a dramatic CCD change would have been approximately 4500 PgC.

Two subsequent numerical modelling studies used both the Walvis Ridge data and the pattern of carbonate sedimentation across the other major ocean basins, to explicitly simulate the carbon-cycle perturbation through the PETM (Panchuk *et al.* 2008; Zeebe *et al.* 2009). The first of these model studies used the Earth-system model GENIE-1 (Grid ENabled Integrated Earth system model), in what was the first pre-quaternary application of a three-dimensional ocean model with full biogeochemical cycling and a spatially resolved coupled sediment model (Panchuk *et al.* 2008). Configured with an equal area grid of resolution of 36 × 36 (comprising 10° increments in longitude but uniform in sine of latitude, giving 3.2° latitudinal increments at the equator increasing to 19.2° in the highest latitude band) and early Eocene bathymetry and palaeogeography (figure 3), GENIE was used to simulate a series of carbon input scenarios representative of the diversity of potential carbon sources. These ranged from purely biogenic methane with an isotopic composition of −60‰ to mantle-derived volcanic CO_2 with a $\delta^{13}C$ signature of −5‰. In each case, the carbon mass input was sufficient to instantaneously decrease the isotopic composition of the combined ocean and atmosphere carbon reservoir by 4‰ and was added uniformly across atmospheric grid cells over 10 kyr. The explicit production of a synthetic sediment column within the GENIE model, whose composition is a function of model bottom-water chemistry and calcium carbonate/organic carbon export production, allows for a direct comparison with the calcium carbonate content and carbon isotopic composition of available deep-sea PETM sediment cores. The sediment model also includes a representation of bioturbation, the intensity of which exerts a critical control on both the shape and magnitude of the PETM dissolution and carbon isotope signals (Ridgwell 2007). This approach allows a direct comparison between the observed and modelled patterns of global marine carbonate sedimentation for both pre-PETM and PETM intervals (figure 3).

The more recent PETM carbon-cycle modelling of Zeebe *et al.* (2009) used the LOSCAR (Long-term Ocean–atmosphere Sediment CArbon cycle Reservoir) box model. LOSCAR uses a three-box (surface, intermediate and deep) representation of each of the major ocean basins. Prior to the PETM, deep-water formation was prescribed to occur in the Southern Ocean and bottom-water temperatures for pre- and peak-PETM were set at 12°C and 16°C, respectively. As in the study of Panchuk *et al.* (2008), carbonate dissolution records were used to constrain the mass of PETM carbon input, in this case based upon comparison between modelled and reconstructed PETM CCD shoaling in the major ocean basins. In order to fit the observed pattern of a relatively prolonged interval of PETM dissolution and CIE, the best-fit scenario consisted of an initial rapid (approx. 5 kyr) carbon input of approximately 3000 PgC followed by an extended (approx. 50 kyr) release of 1480 PgC (figure 4). Combined with the authors' assumed surface ocean CIE of −3‰, this carbon release scenario indicates a source isotopic signature of approximately 50‰, which is consistent with a significant contribution from biogenic methane hydrates (Zeebe *et al.* 2009). It is worth noting that assuming a larger CIE, for example the −4‰ suggested herein, implies an even more ^{13}C-depleted carbon source, unless the magnitude of carbon release also increases.

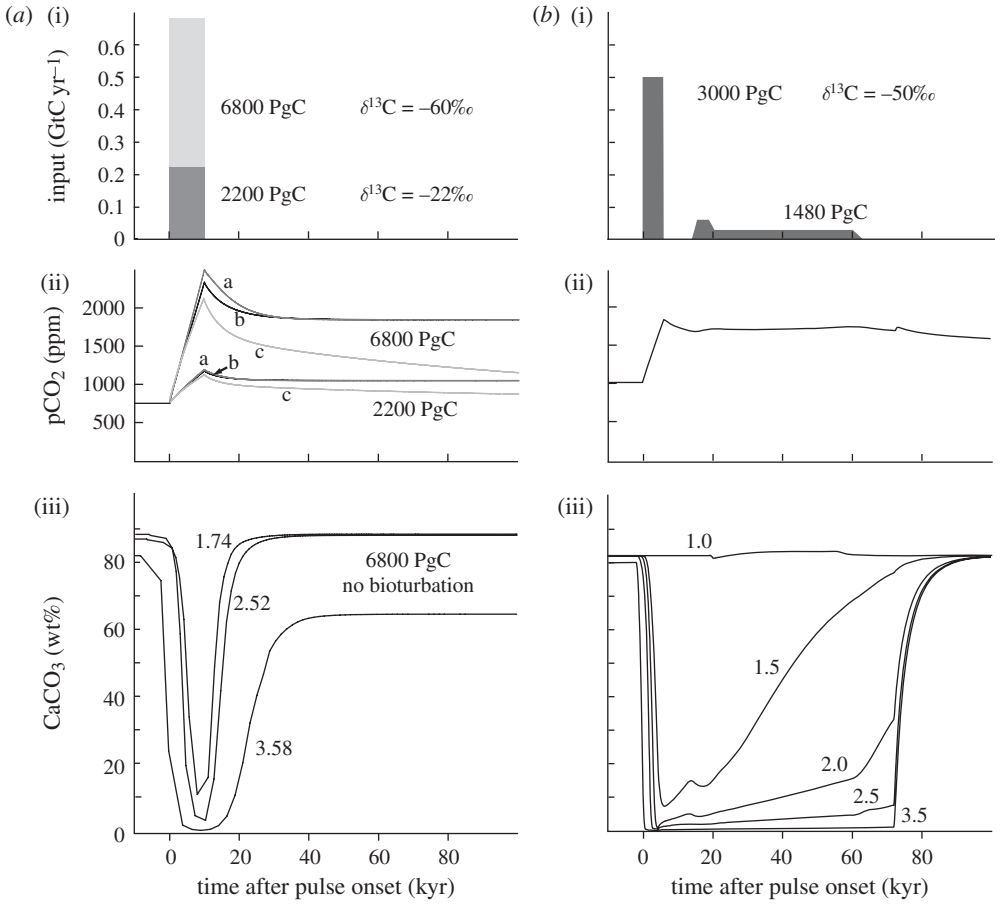

Figure 4. Comparison of time-series results from the GENIE ((*a*) Panchuk *et al.* 2008) and LOSCAR ((*b*) Zeebe *et al.* 2009) models. The GENIE model shows two carbon input scenarios of 2200 and 6800 PgC. The LOSCAR model shows the best-fit carbon input scenario. From top to bottom: (i) carbon input in Gt yr^{-1}; (ii) atmospheric pCO_2 perturbation—for each carbon input scenario in GENIE three curves are shown: a, without bioturbation; b, with bioturbation; c, with bioturbation and a temperature-dependent weathering feedback; (iii) modelled calcium carbonate deposition in the South Atlantic at locations and depths comparable with observed calcium carbonate deposition across the Walvis Ridge depth transect (Zachos *et al.* 2005). GENIE data are from the 6800 PgC input scenario with no bioturbation.

A crucial part of all PETM modelling studies is determining an appropriate initial 'latest Palaeocene' pre-PETM climate and ocean chemistry. In the approach of Panchuk *et al.* (2008), GENIE-1 is initialized with a pre-PETM pCO_2 of 750 ppm, which produces modelled deep-ocean temperatures of approximately 7°C. This is warmer than modern but cooler than the approximately 12°C indicated by benthic foraminiferal $\delta^{18}O$ proxy data (Dunkley Jones *et al.* in preparation). The other key unknowns in the pre-PETM model configuration are global ocean alkalinity and the particulate inorganic to organic carbon rain ratio (PIC : POC ratio). In the absence of suitable proxy data,

Panchuk *et al.* (2008) constrain these variables by running an ensemble of pre-PETM simulations across a range of weathering rates (ocean alkalinity) and spatially uniform PIC : POC rain ratios. Using the observed pattern of pre-PETM deep-sea carbonate sedimentation, Panchuk *et al.* (2008) suggest a pre-PETM CCD of approximately 3500–4000 m in the central equatorial Pacific, Walvis Ridge and Southern Indian Ocean (figure 3). These depths appear to be broadly consistent with the CCD reconstructions of Zeebe *et al.* (2009) and more importantly, within the limits of the data, reproduce the lysocline depth observed at these three data-rich regions (figure 3). The best-fit model calibration to the observed pattern of carbonate deposition requires a PIC : POC ratio of 0.20, which is somewhat higher than estimates of the modern global average of 0.06–0.14 (Sarmiento *et al.* 2002; Ridgwell *et al.* 2007), and a global weathering rate of 35 Pmol HCO_3^- kyr^{-1} to balance the rate of deep-sea calcium carbonate sedimentation. The modelled deep-ocean circulation and associated $\delta^{13}C$ gradients are consistent with available pre-PETM benthic foraminiferal $\delta^{13}C$ data (Nunes & Norris 2006), with decreasing $\delta^{13}C$ from the South to North Atlantic and from the Indian to Pacific Ocean, indicative of a dominant Southern Ocean deep-water source.

In Panchuk *et al.* (2008), the carbon release scenario that was most consistent with the observed pattern of deep-sea carbonate sedimentation at peak-PETM conditions consists of a pulse of 6800 PgC with bioturbation in the Pacific and a cessation of bioturbation in the Atlantic (Panchuk *et al.* 2008). The basin-to-basin variation in bioturbation is required to reproduce the differential dissolution between the Atlantic and the Pacific observed during the event. Carbonate accumulation drops to zero during peak-PETM conditions at even the shallowest of the Walvis Ridge sites in the South Atlantic (i.e. CCD <1500 m), which can be compared with the 20–50 wt% carbonate preserved at 2500 m water depth on Shatsky Rise in the central equatorial Pacific (i.e. CCD >2500 m). Again it should be noted that these best-fit scenarios are consistent with the PETM CCD reconstructions of Zeebe *et al.* (2009), with the only discrepancy being the presence of a small amount of modelled carbonate below their reconstructed CCD in the equatorial Pacific even with a pulse size of 6800 PgC. The absence of bioturbation in the Atlantic increases the intensity of dissolution in surface sediments by removing the resupply of 'old' carbonate from deeper in the sediment column, hence reducing the size of carbon pulse required to produce a zero carbonate layer. There is evidence for such a reduction or cessation of bioturbation in the Atlantic, with the preservation of fine laminations in both equatorial and South Atlantic PETM sediment cores (Erbacher *et al.* 2004; Zachos *et al.* 2004). In contrast, there is clear evidence for continued sediment mixing through the onset of the PETM at shallower sites on Shatsky Rise and Alison Guyot in the Pacific, as well as in the Southern Ocean (Kelly *et al.* 1998; Bralower *et al.* 2002; Thomas *et al.* 2002).

An alternative cause of enhanced dissolution in the Atlantic is an altered deep-ocean circulation, with a major reduction in Southern Ocean deep-water formation and its subsequent ventilation of the South Atlantic (Zeebe & Zachos 2007). During the carbon release experiments of Panchuk *et al.* (2008), the ocean circulation in GENIE does not respond to warming by a reversal or weakening in the Southern Ocean deep-water source. This is consistent with previous ocean modelling studies that only induced a reversed circulation through an explicit

modification of the hydrological cycle and an altered North Atlantic bathymetry (Bice & Marotzke 2002). More recent fully coupled atmosphere–ocean general circulation models (AOGCMs) have, however, reproduced a significant slow down in Southern Ocean deep-water formation in response to greenhouse gas-forced warming alone (Lunt *et al.* submitted). This slowdown is more consistent with the available proxy data (Nunes & Norris 2006) and may help to explain some of the basin-to-basin dissolution variability (Zeebe & Zachos 2007). Any circulation change does not, however, preclude the importance of changes in bioturbation intensity. Indeed, these two effects may represent a coherent change in environmental conditions, with a slowdown in South Atlantic deep-ocean circulation causing a reduction in bottom-water ventilation, dysoxia and the cessation of *in situ* biotic activity.

Although both of these modelling studies indicate a PETM carbon input at least double the initial estimates of 1500–2500 PgC, which were based purely on the CIE and an assumed methane hydrate source (Dickens *et al.* 1995), there are some discrepancies between both the model approaches and their final estimates of carbon release. As Zeebe *et al.* (2009) point out, if a pre-PETM model configuration has an unrealistically deep CCD, this increases the mass of carbonate material available for dissolution at the ocean floor during the PETM acidification event. This in turn will produce a model overestimate of the mass of carbon input required to reproduce the observed carbonate dissolution during the PETM itself—effectively it makes the available oceanic carbonate buffer too large. Although this is an implied criticism of the GENIE model configuration of Panchuk *et al.* (2008), and their proposed pulse size of 6800 PgC, there is no apparent mismatch between their modelled pattern of carbonate sedimentation, lysocline and CCD and the available observations (figure 3). As noted above, however, the PIC : POC ratios and biocarbonate weathering fluxes required in the pre-PETM GENIE calibration are higher than the modern and there may be scope for further tuning of the non-carbonate detrital flux rates (currently a globally uniform value of $0.18\,\mathrm{g\,cm^{-2}\,ky^{-1}}$) to lower total ocean alkalinity and yet retain a similar pattern of observed wt% carbonate sedimentation. There is, however, at least a similar uncertainty involved in the production and use of the CCD reconstructions of Zeebe *et al.* (2009) as a tuning target for modelled pre- and PETM ocean alkalinity. The accurate reconstruction of the CCD, and subsequent inferring of deep-ocean carbonate chemistry, is not straightforward even from modern core-top sediments (Broecker 2008). One advantage of the synthetic sediment cores produced by GENIE is that the model response is translated into a spatially resolved pattern of sediment compositions that can be directly compared with the carbonate content of actual sediment cores. As noted above, this allows detailed model-data comparisons of the depth-dependent pattern of carbonate sedimentation, and hence changes in both the lysocline and CCD, in data-rich regions of the ocean (figure 3).

After the discrepancy in total carbon input (6800 PgC of Panchuk *et al.* (2008) versus the 4480 PgC of Zeebe *et al.* (2009)), the second principal difference in the models concerns the cause of the observed pattern of variation in dissolution intensity between the Atlantic and Pacific basins (Zeebe & Zachos 2007). This differential is not reproducible in the models without some secondary control on the pattern of carbonate dissolution. GENIE runs with and without bioturbation globally suggest that this might be achieved by a cessation of bioturbation at

peak-PETM conditions in the Atlantic while continuing to allow Pacific sediments to be actively mixed (Panchuk *et al.* 2008), although this scenario has not yet been explicitly tested. In LOSCAR, this differential dissolution pattern was achieved by prescribing a weakening of Southern Ocean deep-water formation and an increase in the formation of North Pacific Deep Water during the PETM (Zeebe *et al.* 2009). As discussed above, these two mechanisms have some support from available sediment core and proxy data, and are probably both important aspects of the PETM perturbation.

4. PETM climate sensitivity

One of the critical conclusions made at the end of the modelling study of Zeebe *et al.* (2009) was that a carbon input of 4480 PgC, together with the associated model rise in atmospheric pCO_2 from 1000 to 1700 ppmv (figure 4), implied a climate sensitivity for the PETM considerably above the range of values produced by the IPCC climate model ensemble for the modern climate system. This conclusion relies upon two pieces of information—first their modelled change in atmospheric pCO_2 and second their estimate of PETM surface warming of between 5°C and 9°C (Zeebe *et al.* 2009). In the absence of any reliable proxy data for either the absolute levels or relative changes in atmospheric pCO_2 through the PETM, the only means of assessing the behaviour of the Earth system is through the intercomparison of PETM modelling studies. Within the LOSCAR model runs of Zeebe *et al.* (2009), a set of sensitivity studies indicate that, for a given carbon pulse, the relative increase in pCO_2 through the PETM is relatively insensitive to baseline pre-PETM atmospheric pCO_2 (within the range 500–1500 µatm). This suggests that the carbon pulse size is the critical factor controlling the relative pCO_2 increase. It is, however, difficult to make a direct comparison between the results of GENIE and LOSCAR because not only does the initial atmospheric pCO_2 (and state of global carbon cycling) differ, but so too do the tested scenarios for CO_2 release, both in magnitude and in duration (figure 4).

By assessing and contrasting multiple model studies (here, Panchuk *et al.* (2008) and Zeebe *et al.* (2009)), and with the addition of future carbon-cycle model results, we stand to gain a better understanding of the range of possible pCO_2 variations across the PETM. These carbon-cycle model estimates of PETM pCO_2 can then be compared against climate model simulations and the available palaeotemperature data to reduce uncertainty and target future proxy data collection and model refinements. In this vein, it is worth comparing the modelled pCO_2 changes against a suite of early Eocene configurations (0.4% reduction in solar constant compared with modern; early Eocene topography and bathymetry; ice-free land surface; uniform vegetation) of HadCM3L, one of the UK Met Office's fully coupled AOGCMs (Lunt *et al.* submitted). Model runs have been integrated for greater than 2000 years at $1\times, 2\times, 4\times$ and $6\times$ pre-industrial pCO_2 levels (280 ppmv), providing a reasonable coverage of potential pre- and PETM conditions (range 280–1680 ppmv). A critical finding of this ensemble is that climate sensitivity is relatively constant over this range of pCO_2, at approximately 3.6°C (figure 5). This value can then be used to estimate the global

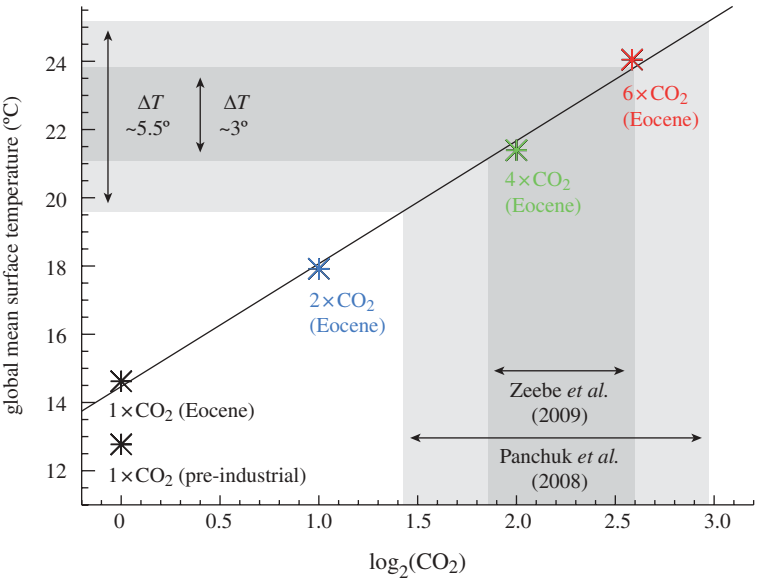

Figure 5. Mean annual surface air temperature as a function of CO_2 forcing across a suite of HadCM3L GCM simulations (Lunt *et al.* submitted). CO_2 forcing is expressed as $\log_2$ of the CO_2 concentration normalized to the pre-industrial level of 280 ppmv. Also plotted are the pCO_2 perturbations of the best-fit carbon release scenarios of Panchuk *et al.* (2008) and Zeebe *et al.* (2009) and the associated estimates of mean annual surface air temperature anomaly predicted for these scenarios by the HadCM3L simulations.

average temperature changes implied by the estimated PETM pCO_2 increases of Panchuk *et al.* (2008) and Zeebe *et al.* (2009) (figure 5); these are 5.5°C and 3°C, respectively.

Finally, we should consider the accuracy and implications of the available surface temperature proxy data. Although Zeebe *et al.* (2009) use the widely quoted range of PETM surface warming of 5–9°C, it is not clear how consistently these proxy data have been interpreted and how representative the specific palaeogeographic locations of these data are of global surface warming. Table 1 shows summary results of a new compilation of the available geochemical palaeotemperature proxy data (Dunkley Jones *et al.* in preparation), which employs a consistent methodology to obtain representative pre-PETM and peak-PETM mean values, as well as using a uniform set of palaeotemperature calculations and calibrations across the available sites. Given that much of these proxy data are subject to issues of stratigraphic completeness and preservational bias, which are discussed in detail in Dunkley Jones *et al.* (in preparation), there are only two sites that indicate warming in excess of 6°C, one from the shelf environment of Wilson Lake and the other from the Southern Ocean ODP Site 690. Although these are arguably two of the better-preserved PETM records, they are also in environments that may be subject to locally enhanced warming, owing either to shallow water depths or to high-latitude amplification of the PETM warming signal. Furthermore, particularly at ODP Site 690, there is a considerable range of variation between proxy

Table 1. Comparison of proxy sea surface temperature estimates across the PETM. Both pre-PETM and peak-PETM temperature estimates based on average values over short stratigraphic intervals immediately before and at peak-PETM conditions. ΔT is the pre- to peak-PETM temperature anomaly based on these proxy estimates. Oxygen isotope temperature estimates are based on HadCM3L modelled δ^{18}Osw values of Tindall *et al.* (in press); Mg/Ca temperature estimates assume a late Palaeocene seawater Mg/Ca ratio of 3.19.

site	reference	proxy method	planktonic foraminifera species used	T (°C) pre-PETM	T (°C) peak-PETM	ΔT
Bass River	John *et al.* (2008)	δ^{18}O	*Acarinina* spp.	27.4	30.4	2.9
	John *et al.* (2008)	δ^{18}O	*Subbotina* spp.	26.5	30.2	3.7
	Sluijs *et al.* (2007)	TEX_{86}	—	28.4	33.8	5.4
Wilson Lake	John *et al.* (2008)	δ^{18}O	*A. soldadoensis*	24.0	32.5	8.5
	John *et al.* (2008)	δ^{18}O	*Subbotina* spp.	25.7	31.9	6.2
	Sluijs *et al.* (2007)	TEX_{86}	—	26.7	34.2	7.5
DSDP 527	Tripati & Elderfield (2004)	δ^{18}O	*A. soldadoensis*	18.4	21.5	3.1
	Tripati & Elderfield (2004)	Mg/Ca	*A. soldadoensis*	~30	~32	~2
	Tripati & Elderfield (2004)	Mg/Ca	*M. subbotinae*	~30	~33	~3
	Tripati & Elderfield (2004)	Mg/Ca	*Subbotina* sp.	~29	~32	~3
ODP 690[a]	Kennett & Stott (1991)	δ^{18}O	*A. praepentacamerata*	13.3	18.4	5.1
	Kennett & Stott (1991)	δ^{18}O	*S. patagonica*	10.5	16.2	5.7
	Thomas *et al.* (2002)	δ^{18}O	*Acarinina* spp.—base PETM	12.7	17.8	5.1
	Thomas *et al.* (2002)	δ^{18}O	*Acarinina* spp.—top PETM	—	21.9	9.1
	Thomas *et al.* (2002)	δ^{18}O	*Subbotina* spp.—base PETM	10.3	16.4	6.0
	Thomas *et al.* (2002)	δ^{18}O	*Subbotina* spp.—top PETM	—	15.8	5.5
ODP 865	Kelly *et al.* (1998)	δ^{18}O	*A. soldadoensis*	23.1	22.5	−0.5
	Tripati & Elderfield (2004)	Mg/Ca	*A. soldadoensis*	31.7	33.3	1.6
	Kelly *et al.* (1998)	δ^{18}O	*M. velascoensis*	22.0	22.0	0.0
	Tripati & Elderfield (2004)		*M. velascoensis*	31.5	32.8	1.3
ODP 1209	Zachos *et al.* (2003)	δ^{18}O	*A. soldadoensis*	20.5	21.3	0.8
	Zachos *et al.* (2003)	Mg/Ca	*A. soldadoensis*	30.3	34.1	3.9
	Zachos *et al.* (2003)	δ^{18}O	*M. velascoensis*	20.7	22.6	1.9
	Zachos *et al.* (2003)	Mg/Ca	*M. velascoensis*	30.6	34.5	3.9
IODP 302-4A (ACEX)	Sluijs *et al.* (2006)	TEX_{86}	—	18.6	22.4	3.9

[a]In the data of Thomas *et al.* (2002) from ODP Site 690 in the Southern Ocean, there is a distinct two-step structure to intra-PETM oxygen isotope data; as a result the peak-PETM interval is analysed here in two sections: from 170.54 to 170.26 mbsf ('base PETM') and from 170.21 to 169.84 mbsf ('top PETM'). For further details of all analyses, see Dunkley Jones *et al.* (in preparation).

measurements on different planktonic foraminifera species, with the average being approximately 6°C. It should be clear from the limited geographic spread, quality and quantity of available PETM palaeotemperature proxy data that we are some way from the reliable estimate of global mean surface warming necessary to constrain PETM climate sensitivity with confidence. At this stage, a conservative interpretation of the proxy data would indicate a pattern of global surface warming in the range of 5–6°C rather than the 5–9°C quoted by Zeebe *et al.* (2009). This is also consistent with available estimates of warming from the terrestrial record: 3–7°C from carbonate soil nodule δ^{18}O (Bowen *et al.* 2001; Koch *et al.* 2003); 4–6°C from δ^{18}O of biogenic phosphate (Fricke *et al.* 1998; Fricke & Wing 2004); and approximately 5°C from leaf margin analysis (Wing *et al.* 2005).

The challenge to our current understanding of climate sensitivity presented by Zeebe *et al.* (2009) thus comes from their estimate of the PETM carbon pulse size, which is at the lower range of the plausible carbon-cycle models of the PETM, combined with an interpretation of the temperature anomaly that leans towards the higher end of available proxy data. An alternative scenario, using the PETM carbon pulse modelled by Panchuk *et al.* (2008), together with a more conservative interpretation of the palaeotemperature proxy data as representing a 5–6°C warming, places the PETM climatic perturbation within the range of state-of-the art climate model simulations.

5. Concluding remarks

Although a great deal is now known about the rate, timings and global nature of the PETM event, critical uncertainties still remain about the cause of the carbon-cycle perturbation and the details of the climate system response. On consideration of the size and global expression of the negative CIE, it still appears likely that a large-scale release of methane hydrate contributed substantially to the massive input of carbon to the exogenic reservoir. With improved estimates of the mass of PETM carbon input, now within the range of approximately 4000–7000 PgC, it is difficult to ascribe all of this carbon to a methane hydrate source. Even in the modern system, the best estimates of the hydrate reservoir are approximately 500–2500 PgC (Milkov 2004), and in the significantly warmer Palaeogene world, the size of the hydrate stability zone should have been reduced not increased. A plausible scenario, consistent with proxy evidence for warming immediately prior to the onset of the CIE (Sluijs *et al.* 2007), is that a rapid CO_2-driven warming—the cause of which is still unknown—subsequently triggered the large-scale dissociation of methane hydrates and the injection of massive quantities of light carbon into the ocean–atmosphere system. That methane hydrates may have operated as a positive feedback mechanism to rapid global warming, even in the warmer ocean/smaller hydrate reservoir Palaeogene world, leaves open the question of what role hydrate-bound carbon will play in the coming centuries of Earth history.

We are grateful for the constructive comments of two anonymous reviewers. This work was supported by Natural Environment Research Council (NERC) grant *The Dynamics of the Palaeocene/Eocene Thermal Maximum*, part of the QUEST research programme.

References

Andres, R. J., Marland, G., Boden, T. & Bischof, S. 1993 Carbon dioxide emissions from fossil fuel combustion and cement manufacture, 1751–1991, and an estimate of their isotopic composition and latitudinal distribution. In *The carbon cycle* (eds T. M. L. Wigley & D. S. Schimel), pp. 53–62. Cambridge, MA: Cambridge University Press.

Archer, D., Kheshgi, H. & Maier-Reimer, E. 1997 Multiple timescales for neutralization of fossil fuel CO_2. *Geophys. Res. Lett.* **24**, 405–408. (doi:10.1029/97GL00168)

Bice, K. L. & Marotzke, J. 2002 Could changing ocean circulation have destabilized methane hydrate at the Paleocene/Eocene boundary? *Paleoceanography* **17**, 1018. (doi:10.1029/2001PA000678)

Bowen, G. J., Koch, P. L., Gingerich, P. D., Norris, R. D., Bains, S. & Corfield, R. M. 2001 Refined isotope stratigraphy across the continental Paleocene–Eocene boundary at Polecat Bench in the northern Bighorn Basin. In *Paleocene–Eocene stratigraphy and biotic change in the Bighorn and Clarks Fork Basins, Wyoming*, vol. 33 (ed. P. D. Gingerich), pp. 73–88. Ann Arbor, MI: University of Michigan.

Bowen, G. J., Beerling, D. J., Koch, P. L., Zachos, J. C. & Quattlebaum, T. 2004 A humid climate state during the Palaeocene/Eocene thermal maximum. *Nature* **432**, 495–499. (doi:10.1038/nature03115)

Bralower, T. J., Thomas, D. J., Zachos, J. C., Hirschmann, M. M., Röhl, U., Sigurdsson, H., Thomas, E. & Whitney, D. L. 1997 High-resolution records of the late Paleocene thermal maximum and circum-Caribbean volcanism: is there a causal link? *Geology* **25**, 963–966. (doi:10.1130/0091-7613(1997)025<0963:HRROTL>2.3.CO;2)

Bralower, T. J. *et al.* 2002 *Proceedings of the ocean drilling program, initial reports, 198.* College Station, TX: Ocean Drilling Program.

Broecker, W. S. 2008 A need to improve reconstructions of the fluctuations in the calcite compensation depth over the course of the Cenozoic. *Paleoceanography* **23**, PA1204. (doi:10.1029/2007PA001456).

Broecker, W. S., Li, Y.-H. & Peng, T. H. 1971 Carbon dioxide—man's unseen artifact. In *Impingement of man on the oceans* (ed. D. W. Hood), pp. 287–324. New York, NY: John Wiley.

Broecker, W. S., Lao, Y., Klas, M., Clark, E., Bonani, G., Ivy, S. & Chen, C. 1993 A search for an early Holocene $CaCO_3$ preservation event. *Paleoceanography* **8**, 333–339. (doi:10.1029/93PA00423)

Dickens, G. R. 2003 Rethinking the global carbon cycle with a large, dynamic and microbially mediated gas hydrate capacitor. *Earth Planet. Sci. Lett.* **213**, 169–183. (doi:10.1016/S0012-821X(03)00325-X)

Dickens, G. R., O'Neil, J. R., Rea, D. K. & Owen, R. M. 1995 Dissociation of oceanic methane hydrate as a cause of the carbon isotope excursion at the end of the Paleocene. *Paleoceanography* **10**, 965–971. (doi:10.1029/95PA02087)

Dunkley Jones, T., Lunt, D. J., Schmidt, D. N., Chun, C., Tindall, J., Maslin, M., Ridgwell, A. & Valdes, P. J. In preparation. A review of the Paleocene–Eocene thermal maximum temperature anomaly.

Ehhalt, D. *et al.* 2001 Atmospheric chemistry and greenhouse gases. In *Climate change 2001: the scientific basis. Contribution of Working Group I to the Third Assessment Report of the Intergovernmental Panel on Climate Change* (eds J. T. Houghton, Y. Ding, D. J. Griggs, M. Noguer, P. J. van der Linden, X. Dai, K. Maskell & C. A. Johnson), pp. 239–287. Cambridge, MA: Cambridge University Press.

Erbacher, J. *et al.* 2004 *Proceedings of the ocean drilling program, initial reports, 207.* College Station, TX: Ocean Drilling Program.

Fricke, H. C. & Wing, S. L. 2004 Oxygen isotope and paleobotanical estimates of temperature and δ^{18}O-latitude gradients over North America during the early Eocene. *Am. J. Sci.* **304**, 612–635. (doi:10.2475/ajs.304.7.612)

Fricke, H. C., Clyde, W. C., O'Neil, J. R. & Gingerich, P. D. 1998 Evidence for rapid climate change in North America during the latest Paleocene thermal maximum: oxygen isotope compositions

of biogenic phosphate from the Bighorn Basin (Wyoming). *Earth Planet. Sci. Lett.* **160**, 193–208. (doi:10.1016/S0012-821X(98)00088-0)

Goodwin, P. & Ridgwell, A. In press. Ocean–atmosphere partitioning of anthropogenic carbon dioxide on multi-millenial timescales. *Global Biogeochem. Cycles*. (doi:10.1029/2008GB003449)

Handley, L., Pearson, P. N., McMillan, I. K. & Pancost, R. D. 2008 Large terrestrial and marine carbon and hydrogen isotope excursions in a new Paleocene/Eocene boundary section from Tanzania. *Earth Planet. Sci. Lett.* **275**, 17–25. (doi:10.1016/j.epsl.2008.07.030)

Higgins, J. A. & Schrag, D. P. 2006 Beyond methane: towards a theory for the Paleocene–Eocene thermal maximum. *Earth Planet. Sci. Lett.* **245**, 523–537. (doi:10.1016/j.epsl.2006.03.009)

John, C. M., Bohaty, S. M., Zachos, J. C., Sluijs, A., Gibbs, S., Brinkhuis, H. & Bralower, T. J. 2008 North American continental margin records of the Paleocene–Eocene thermal maximum: implications for global carbon and hydrological cycling. *Paleoceanography* **23**, PA2217. (doi:10.1029/2007PA001465)

Katz, M. E., Pak, D. K., Dickens, G. R. & Miller, K. G. 1999 The source and fate of massive carbon input during the latest Paleocene thermal maximum. *Science* **286**, 1531–1533. (doi:10.1126/science.286.5444.1531)

Katz, M. E., Cramer, B. S., Mountain, G. S., Katz, S. & Miller, K. G. 2001 Uncorking the bottle: what triggered the Paleocene/Eocene thermal maximum methane release? *Paleoceanography* **16**, 549–562. (doi:10.1029/2000PA000615)

Kelly, D. C., Bralower, T. J. & Zachos, J. C. 1998 Evolutionary consequences of the latest Paleocene thermal maximum for tropical planktonic foraminifera. *Palaeogeogr. Palaeoclimatol. Palaeoecol.* **141**, 139–161. (doi:10.1016/S0031-0182(98)00017-0)

Kennett, J. P. & Stott, L. D. 1991 Abrupt deep-sea warming, palaeoceanographic changes and benthic extinctions at the end of the Paleocene. *Nature* **353**, 225–229. (doi:10.1038/353225a0)

Kent, D. V., Cramer, B. S., Lanci, L., Wang, D., Wright, J. D. & van der Voo, R. 2003 A case for a comet impact trigger for the Paleocene/Eocene thermal maximum and carbon isotope excursion. *Earth Planet. Sci. Lett.* **211**, 13–26. (doi:10.1016/S0012-821X(03)00188-2)

Koch, P. L., Clyde, W. C., Hepple, R. P., Fogel, M. L., Wing, S. L. & Zachos, J. C. 2003 Carbon and oxygen isotope records from paleosols spanning the Paleocene–Eocene boundary, Bighorn Basin, Wyoming. In *Causes and consequences of globally warm climates in the early Paleogene*, vol. 369 (eds S. L. Wing, P. D. Gingerich, B. Schmitz & E. Thomas), pp. 49–64. Boulder, CO: Geological Society of America.

Kohfeld, K. E. & Ridgwell, A. 2009 Glacial–interglacial variability in atmospheric CO_2. In *Surface ocean—lower atmosphere processes*, vol. 187 (eds C. Le Quéré & E. S. Saltzman), pp. 251–286. Washington, DC: American Geophysical Union.

Kraus, M. J. & Riggins, S. 2007 Transient drying during the Paleocene–Eocene thermal maximum (PETM): analysis of paleosols in the bighorn basin, Wyoming. *Palaeogeogr. Palaeoclimatol. Palaeoecol.* **245**, 444–461. (doi:10.1016/j.palaeo.2006.09.011)

Kump, L. R., Bralower, T. J. & Ridgwell, A. 2009 Ocean acidification in deep time. *Oceanography* **22**, 94–107.

Kurtz, A. C., Kump, L. R., Arthur, M. A., Zachos, J. C. & Paytan, A. 2003 Early Cenozoic decoupling of the global carbon and sulfur cycles. *Paleoceanography* **18**, 1090. (doi:10.1029/2003PA000908)

Kvenvolden, K. A. 1993 Gas hydrates—geological perspective and global change. *Rev. Geophys.* **31**, 173–187. (doi:10.1029/93RG00268)

Lunt, D. J., Valdes, P. J., Dunkley Jones, T., Ridgwell, A., Haywood, A. M., Schmidt, D. N., Marsh, R. & Maslin, M. Submitted. CO_2 driven ocean circulation changes as an amplifier of PETM destabilization.

Maslin, M. A. & Thomas, E. 2003 Balancing the deglacial global carbon budget: the hydrate factor. *Quat. Sci. Rev.* **22**, 1729–1736. (doi:10.1016/S0277-3791(03)00135-5)

Maslin, M., Owen, M., Betts, R., Day, S., Dunkley Jones, T. & Ridgwell, A. 2010 Gas hydrates: past and future geohazard? *Phil. Trans. R. Soc. A* **368**, 2369–2393. (doi:10.1098/rsta.2010.0065)

McCarren, H., Thomas, E., Hasegawa, T., Röhl, U. & Zachos, J. C. 2008 Depth dependency of the Paleocene–Eocene carbon isotope excursion: paired benthic and terrestrial biomarker records

(Ocean Drilling Program Leg 208, Walvis Ridge). *Geochem. Geophys. Geosyst.* **9**, Q10008. (doi:10.1029/2008GC002116)

Milkov, A. V. 2004 Global estimates of hydrate-bound gas in marine sediments: how much is really out there? *Earth Sci. Rev.* **66**, 183–197. (doi:10.1016/j.earscirev.2003.11.002)

Nunes, F. & Norris, R. D. 2006 Abrupt reversal in ocean overturning during the Palaeocene/Eocene warm period. *Nature* **439**, 60–63. (doi:10.1038/nature04386)

Pagani, M., Pedentchouk, N., Huber, M., Sluijs, A., Schouten, S., Brinkhuis, H., Sinninghe Damsté, J. S., Dickens, G. R. & Expedition 302 Scientists. 2006 Arctic hydrology during global warming at the Palaeocene/Eocene thermal maximum. *Nature* **442**, 671–675. (doi:10.1038/nature05043)

Panchuk, K., Ridgwell, A. & Kump, L. R. 2008 Sedimentary response to Paleocene-Eocene thermal maximum carbon release: a model-data comparison. *Geology* **36**, 315–318. (doi:10.1130/G24474A.1)

Paull, C. K., Brewer, P. G., Ussler, W., Peltzer, E. T., Rehder, G. & Clague, D. 2003 An experiment demonstrating that marine slumping is a mechanism to transfer methane from seafloor gas-hydrate deposits into the upper ocean and atmosphere. *Geo-Mar. Lett.* **22**, 198–203. (doi:10.1007/S00367-002-0113-y)

Prentice, I. C. *et al.* 2001 The carbon cycle and atmospheric carbon dioxide. In *Climate change 2001: the scientific basis. Contribution of Working Group I to the Third Assessment Report of the Intergovernmental Panel on Climate Change* (eds J. T. Houghton, Y. Ding, D. J. Griggs, M. Noguer, P. J. van der Linden, X. Dai, K. Maskell & C. A. Johnson), pp. 183–237. Cambridge, MA: Cambridge University Press.

Ridgwell, A. 2007 Interpreting transient carbonate compensation depth changes by marine sediment core modeling. *Paleoceanography* **22**, PA4102. (doi:10.1029/2006PA001372)

Ridgwell, A. & Edwards, U. 2007 Geological carbon sinks. In *Greenhouse gas sinks* (eds D. Reay, C. N. Hewitt, K. Smith & J. Grace), pp. 74–97. Wallingford, CT: CAB International.

Ridgwell, A. & Zeebe, R. E. 2005 The role of the global carbonate cycle in the regulation and evolution of the Earth system. *Earth Planet. Sci. Lett.* **234**, 299–315. (doi:10.1016/j.epsl.2005.03.006)

Ridgwell, A. J., Hargreaves, J. C., Edwards, N. R., Annan, J. D., Lenton, T. M., Yool, A., Marsh, R. & Watson, A. J. 2007 Marine geochemical data assimilation in an efficient Earth system model of global biogeochemical cycling. *Biogeosciences* **4**, 87–104.

Sarmiento, J. L., Dunne, J. P., Gnanadesikan, A., Key, R. M., Matsumoto, K. & Slater, R. 2002 A new estimate of the $CaCO_3$ to organic carbon export ratio. *Global Biogeochem. Cycles* **16**, 1107. (doi:10.1029/2002GB001919)

Sluijs, A. *et al.* & the Expedition 302 Scientists. 2006 Subtropical Arctic Ocean temperatures during the Palaeocene/Eocene thermal maximum. *Nature* **441**, 610–613. (doi:10.1038/nature04668)

Sluijs, A. *et al.* 2007 Environmental precursors to rapid light carbon injection at the Palaeocene/Eocene boundary. *Nature* **450**, 1218–1221. (doi:10.1038/nature06400)

Storey, M., Duncan, R. A. & Swisher, C. C. 2007 Paleocene–Eocene thermal maximum and the opening of the northeast Atlantic. *Science* **316**, 587–589. (doi:10.1126/science.1135274)

Svensen, H., Planke, S., Malthe-Sorenssen, A., Jamtveit, B., Myklebust, R., Eidem, T. R. & Rey, S. S. 2004 Release of methane from a volcanic basin as a mechanism for initial Eocene global warming. *Nature* **429**, 542–545. (doi:10.1038/nature02566)

Thomas, E. 2007 Cenozoic mass extinctions in the deep sea: what disturbs the largest habitat on Earth? In *Large ecosystem perturbations: causes and consequences*, vol. 424 (eds S. Monechi, R. Coccioni & M. Rampino), pp. 1–23. Boulder, CO: Geological Society of America.

Thomas, D. J., Zachos, J. C., Bralower, T. J., Thomas, E. & Bohaty, S. 2002 Warming the fuel for the fire: evidence for the thermal dissociation of methane hydrate during the Paleocene–Eocene thermal maximum. *Geology* **30**, 1067–1070. (doi:10.1130/0091-7613(2002)030<1067:WTFFTF>2.0.CO;2)

Tindall, J., Flecker, R., Valdes, P. J., Schmidt, D. N., Markwick, P. J. & Harris, J. In press. Modelling the oxygen isotope distribution of ancient seawater using a coupled ocean-atmosphere GCM: implications for reconstructing early Eocene climate. *Earth Planet. Sci. Lett.* (doi:10.1016/j.epsl.2009.12.049)

Tripati, A. K. & Elderfield, H. 2004 Abrupt hydrographic changes in the equatorial Pacific and subtropical Atlantic from foraminiferal Mg/Ca indicate greenhouse origin for the thermal maximum at the Paleocene–Eocene Boundary. *Geochem. Geophys. Geosyst.* **5**, Q02006. (doi:10.1029/2003GC000631)

Valentine, D. L., Blanton, D. C., Reeburgh, W. S. & Kastner, M. 2001 Water column methane oxidation adjacent to an area of active hydrate dissociation. *Geochem. Cosmochem. Acta* **65**, 2633–2640. (doi:10.1016/S0016-7037(01)00625-1)

Wing, S. L., Harrington, G. J., Smith, F. A., Bloch, J. I., Boyer, D. M. & Freeman, K. H. 2005 Transient floral change and rapid global warming at the Paleocene–Eocene boundary. *Science* **310**, 993–996. (doi:10.1126/science.1116913)

Zachos, J. C., Wara, M. W., Bohaty, S., Delaney, M. L., Petrizzo, M. R., Brill, A., Bralower, T. J. & Premoli-Silva, I. 2003 A transient rise in tropical sea surface temperature during the Paleocene–Eocene thermal maximum. *Science* **302**, 1551–1554. (doi:10.1126/science.1090110)

Zachos, J. C., Kroon, D., Blum, P. *et al.* 2004 *Proceedings of the ocean drilling program, initial reports, 208*. College Station, TX: Ocean Drilling Program.

Zachos, J. C., *et al.* 2005 Rapid acidification of the ocean during the Paleocene–Eocene thermal maximum. *Science* **308**, 1611–1615. (doi:10.1126/science.1109004)

Zachos, J. C., Schouten, S., Bohaty, S., Quattlebaum, T., Sluijs, A., Brinkhuis, H., Gibbs, S. J. & Bralower, T. J. 2006 Extreme warming of mid-latitude coastal ocean during the Paleocene–Eocene thermal maximum: inferences from TEX86 and isotope data. *Geology* **34**, 737–740. (doi:10.1130/G22522.1)

Zachos, J. C., Bohaty, S. M., John, C. M., McCarren, H., Kelly, D. C. & Nielsen, T. 2007 The Palaeocene–Eocene carbon isotope excursion: constraints from individual shell planktonic foraminifer records. *Phil. Trans. R. Soc. A* **365**, 1829–1842. (doi:10.1098/rsta.2007.2045)

Zachos, J. C., Dickens, G. R. & Zeebe, R. E. 2008 An early Cenozoic perspective on greenhouse warming and carbon-cycle dynamics. *Nature* **451**, 279–283. (doi:10.1038/nature06588)

Zeebe, R. E. & Zachos, J. C. 2007 Reversed deep-sea carbonate ion basin gradient during Paleocene–Eocene thermal maximum. *Paleoceanography* **22**, PA3201. (doi:10.1029/2006PA001395)

Zeebe, R. E., Zachos, J. C. & Dickens, G. R. 2009 Carbon dioxide forcing alone insufficient to explain Palaeocene–Eocene thermal maximum warming. *Nat. Geosci.* **2**, 576–580. (doi:10.1038/ngeo578)